coatings

MDPI

Article

Supplementary Information: Enhanced the Efficiency of Photocatalytic Degradation of Methylene Blue by Construction of Z-Scheme g-C_3N_4/$BiVO_4$ Heterojunction

Xiong Zhang [1,2,3], Minjin Li [1], Cheng Liu [1], Zhiyong Zhang [1,*], Fuchun Zhang [2,3] and Qiaoping Liu [1,2]

[1] School of Information Science Technology, Northwest University, Xi'an 710127, China; zhangxiong0911@163.com (X.Z.); minjli@163.com (M.L.); lc@nwu.edu.cn (C.L.); liuqioaping1211@126.com (Q.L.)
[2] School of Physics and Electronic Information, Yan'an University, Yan'an 716000, China; yadxzfc@163.com
[3] Shaanxi Key Laboratory of Intelligent Processing for Big Energy Data, Yan'an University, Yan'an 716000, China
* Correspondence: zhangzy@nwu.edu.cn

Citation: Zhang, X.; Li, M.J.; Liu, C.; Zhang, Z.Y.; Zhang, F.C.; Liu, Q.P. Enhanced the Efficiency of Photocatalytic Degradation of Methylene Blue by Construction of Z-Scheme g-C_3N_4/$BiVO_4$ Heterojunction. *Coatings* **2021**, *11*, 1027. https://doi.org/10.3390/coatings11091027

Academic Editor: Alexandru Enesca

Received: 31 July 2021
Accepted: 20 August 2021
Published: 26 August 2021

Publisher's Note: MDPI stays neutral with regard to jurisdictional claims in published maps and institutional affiliations.

Copyright: © 2021 by the authors. Licensee MDPI, Basel, Switzerland. This article is an open access article distributed under the terms and conditions of the Creative Commons Attribution (CC BY) license (http://creativecommons.org/licenses/by/4.0/).

1. FT-IR

The FT-IR spectra of CN, BVO, and 1.0-CN/BVO heterojunction are shown in Figure S1. For pristine monoclinic BVO, the vibrational band at 731 cm^{-1} was due to asymmetric stretching vibration of the ν3 (VO_4) [1]. The absorption band of the pristine CN at 1612 cm^{-1} was indexed to the C-N stretching vibration modes. The three vibrational bands at 1573, 1501, and 1418 cm^{-1} were indicative of the typical stretching mode of CN heterocycle. The bands at 1320 and 1258 cm^{-1} were assigned to the stretching vibration of connected units of C–N–(–C)–C or C–NH–C [2], respectively. The band at 828 cm^{-1} was belong to the plane skeletal bending modes of the triazine cycles. The broad absorption band within 3100–3300 cm^{-1} was associated with the N–H stretching vibration of the residual NH group, which is the residual amino with incomplete polymerization after the calcining process or O–H stretching associated with adsorbed water [3]. It is obvious that the primary bands of CN and BVO were included in hybrid photocatalysts, implying that the g-C_3N_4/$BiVO_4$ heterojunction was fabricated successfully.

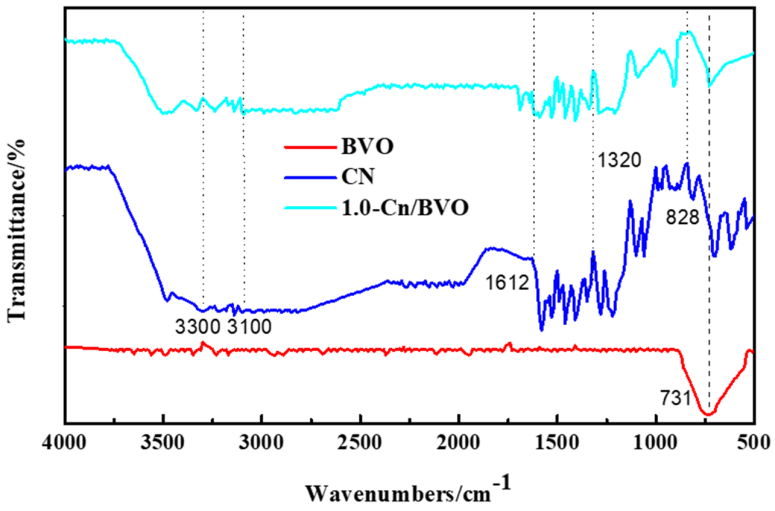

Figure S1. FT-IR spectra of pristine CN, pristine BVO, and 1.0-CN/BVO.

2. Photocatalytic Degradation Performance

In order to effectively evaluate the photocatalytic degradation of MB by 1.0-CN/BVO under visible light, we examined the photolysis of MB in the absence of the catalyst. As exhibited in Figure S2, the photolysis of MB changed slightly during light irradiation in the absence of the catalyst. In addition, the photocatalytic performance of a certain amount of catalyst for different concentrations of MB solution and the different amounts of catalyst for a certain concentration of MB solution were investigated. The results show that the higher the ratio of catalyst to MB concentration, the higher the photocatalytic efficiency.

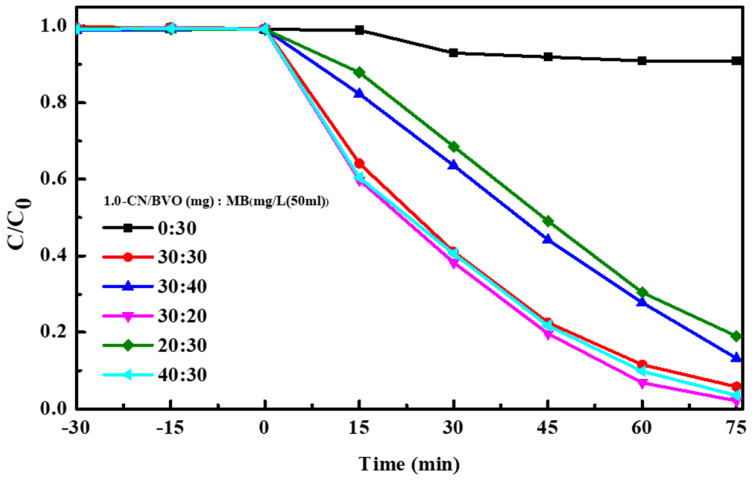

Figure S2. Under visible light irradiation, the removal rate of MB with different concentrations of 1.0-CN/BVO; check the photolysis of MB in the absence of the catalyst.

3. Active Species Trapping Experiments

In order to get insights into the photocatalytic mechanism, the active species trapping experiments were carried out to examine the effective active species during the photodegradation process. The quenching agents, including 1,4-benzoquinone (BQ), potassium iodide (KI), and isopropanol (IPA) were added into the 1.0-CN/BVO system as a superoxide radical (0_2^-), holes (h^+), and hydroxyl radical (OH) scavenger, respectively. As depicted in Figure S3, the photodegradation rates of MB were apparently depressed from 99.3% to 23%, 77%, and 17% when BQ, IPA, and KI were added into the reaction system, respectively. The results suggested that all the radicals of$\cdot 0_2^-$, OH, and h^+ worked in MB degradation over 1.0-CN/BVO, and the$\cdot 0_2^-$ and h^+ played the most dominate roles in photocatalysis reaction.

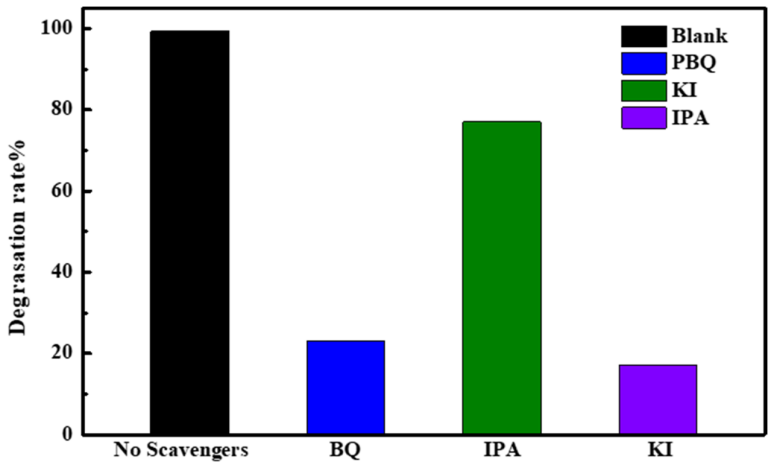

Figure S3. Trapping experiments of active species during the photocatalytic degradation of MB over 1.0-CN/BVO sample under visible light irradiation.

Table S1. The photocatalytic performance and catalytic efficiency were compared with other C_3N_4, $BiVO_4$, and $C_3N_4/BiVO_4$ materials.

Photocatalyst (mg)	Reaction Parameters	Photocatalytic Application	Time and Rate of Photocatalytic Activity (Time (min)/ Rate (%))	Ref
g-C_3N_4 (100 mg)	300 W Xe lamp, cut-off filter (420 nm) + H_2O_2 (2ml)	Degradation of MB (100 mL, 100 mg/L)	120 min/39%	[4]
$BiVO_4$ (10 mg)	1000 W Xe lamp, cut-off filter (420 nm)	Degradation of MB (30 mL, 20 mg/L)	60 min/90%	[5]
g-C_3N_4/$BiVO_4$ (50 mg)	500 W Xe lamp, cut-off filter (420 nm)	Degradation of MB (50 mL, 10 mg/L)	120 min/90%	[6]
$BiVO_4$/g-C_3N_4 (30 mg)	50 W LED, cut-off filter (410 nm)	Degradation of MB (30 mL, 20 mg/L)	60 min/97%	[7]
g-C_3N_4/$BiVO_4$ (30 mg)	100 W LED, cut-off filter (410 nm)	Degradation of MB (50 mL, 30 mg/L)	75 min/93%	This work

References

1. Frost, R.L.; Henry, D.A.; Weier, M.L.; Martens, W. Raman spectroscopy of three polymorphs of $BiVO_4$: clinobisvanite, dreyerite and pucherite, with comparisons to $(VO_4)_3$-bearing minerals: namibite, pottsite and schumacherite. *J. of Raman Spectrosc.* **2006**, *37*, 722–732.
2. Zhou, S.; Liu, Y.; Li, J.; Wang, Y.; Jiang, G.; Zhao, Z.; Wang, D.; Duan, A.; Liu, J.; Wei, Y. Facile in situ synthesis of graphitic carbon nitride (g-C_3N_4)-N-TiO_2 heterojunction as an efficient photocatalyst for the selective photoreduction of CO_2 to CO. *Appl. Catal. B: Environ.* **2014**, *158–159*, 20–29.
3. Zhao, Y.; Liu, Z.; Chu, W.; Song, L.; Zhang, Z.; Yu, D.; Tian, Y.; Xie, S.; Sun, L. Large-scale synthesis of nitrogen-rich carbon nitride microfibers by using graphitic carbon nitride as precursor. *Adv. Mater.* **2008**, *20*, 1777–1781.
4. Feng, J.; Chen, T.; Liu, S.; Zhou, Q.; Ren, Y.; Lv, Y.; Fan, Z. Improvement of g-C_3N_4 photocatalytic properties using the Hummers method. *J Colloid Interface Sci.* **2016**, *479*, 1–6.
5. Kamble, G.S.; Ling, Y.C. Solvothermal synthesis of facet-dependent $BiVO_4$ photocatalyst with enhanced visible-light-driven photocatalytic degradation of organic pollutant: assessment of toxicity by zebrafish embryo. *Sci Rep.* **2020**, *10*, 12993.
6. Cheng, J.; Yan, X.; Mo, Q.; Liu, B.; Wang, J.; Yang, X.; Li, L. Facile synthesis of g-C_3N_4/$BiVO_4$ heterojunctions with enhanced visible light photocatalytic performance. *Ceram. Int.* **2017**, *43*, 301–307.
7. Wang, Z.; Lv, J.; Zhang, J.; Dai, K.; Liang, C. Facile synthesis of Z-scheme $BiVO_4$/porous graphite carbon nitride heterojunction for enhanced visible-light-driven photocatalyst. *Appl. Surf. Sci.* **2018**, *430*, 595–602.